Compatible Hole Channel Mobility and Hole Quantum Correction Models for the TCAD optimization of Nanometer Scale PMOSFETs

C. D. Nguyen, C. Jungemann, B. Neinhüs, B. Meinerzhagen, J. Sedlmeir* and W. Molzer*

Institut für Theoretische Elektrotechnik und Mikroelektronik
Universität Bremen, Otto-Hahn-Allee, 28334 Bremen, Germany, cdong@item.uni-bremen.de
* Infineon Technologies AG, CL TD SIM, 81730 München

ABSTRACT

This paper presents a quantum correction model for the hole inversion layer based on the Improved Modified Local Density Approximation (IMLDA) and a corresponding channel mobility model compatible to the IMLDA quantum corrected spatial p-density and field distributions. The combination of both models correctly describes the effects of hole inversion layer quantization on threshold voltage and current without increasing the computation time. The IMLDA model agrees well with results of the self-consistent solution of Schrödinger and Poisson equations (SE/PE) for a wide range of temperatures and doping concentrations. The new mobility model is compatible to the IMDLA quantum corrected charge densities and agrees well with experimental mobility data within the same range of temperatures and doping densities. A big advantage of the IMLDA model and the new mobility model is their low computational cost and their numerical robustness, because both depend only locally on field, doping and temperature.

Keywords: MOS devices, Quantization effects, Inversion layer

1 INTRODUCTION

Due to the smaller oxide thickness and higher channel doping used in modern CMOS-technologies, quantum effects cannot be neglected in device simulations of MOS transistors. The accurate description of the quantum effects additionally requires the solution of the SE while calculating the inversion layer charge density which is very important for the determination of key parameters of MOS transistors such as the threshold voltage. However, the self-consistent solution of the SE/PE, which would be the ideal solution here, increases the computation time and degrades the algorithmic flexibility of the device simulators substantially. Therefore, simplified models that fit better into the overall algorithmic framework of the device simulator and approximately describe the size quantization effect with an affordable increase of computation time [1]–[4] were developed. The model proposed in [1] provides an accurate modeling for the inversion layer density, but it is non-local in the electrostatic potential. The numerically more complex density gradient method even includes aspects of quantum transports, but leads to convergence problems and substantially increased CPU-times [2]. The models in [3], [4] inaccurately describe the inversion layer charge density, since they are based on the self-consistent solution of SE/PE without accounting for the warped valence band structure. Therefore, the IMLDA model for holes which is numerically robust and accurate for device simulations was developed based on the model in [5].

With the strong modification of the spatial hole density distribution near the Si/SiO_2 interface due to size quantization, the previously developed local mobility models based on the classical charge distribution (e.g [6], [7]) cannot be used for the simulation of the drain current. Moreover, the local hole mobilities of Ref. [6], [7] are only accurate for room temperature. Therefore, the new local hole mobility model which is applicable for a wide range of temperatures and substrate doping concentrations was developed similar to the case of electrons [8]. The mobility model developed in this work is strictly local in the solution variables of the balance equations. Furthermore, in conjunction with the IMLDA model it is not detrimental to the convergence properties, the CPU efficency, and the robustness of the device simulator.

2 IMLDA MODEL

For the development of the IMLDA model, reference data were produced using the self-consistent solution of the SE/PE for a large range of temperatures and doping. These data were then used for the parameter fitting of the IMLDA model. For electrons, the conduction band structure can be described successfully in the SE on the basis of parabolic spherical bands and constant effective masses [9]–[11] (one-band effective mass approximation, EMA). For holes, the description of the valence band structure in the SE with the EMA [4] is not reliable, since the valence band structure is much more complicated compared to the conduction band. In [12] an algorithm was presented for the self-consistent solution of the SE/PE with a complete description of the valence band structure in the SE using the $k \cdot p$-method (full-band SE/PE solver $nextnano^3$). However, for the production of a large quantity of reference data, the use of the SE/PE solver [12] would require an enormous amount of computation time. Additionally, this SE/PE solver works only for room temperature. In contrast, the EMA SE/PE solver needs much less computation time, so that this simulator would be suitable for the production of the reference data. In order to keep the EMA SE/PE solver as reference model for IMLDA development,

the effective masses of the EMA SE/PE solver [11] were fitted in such a manner that the simulation results of the full-band SE/PE solver were well reproduced. As a matching criterion the inversion charge density was used.

Similarly to Ref. [5] the IMLDA model for holes reads:

$$p(z) = n_{i,0} \cdot qc \cdot \exp\left(\frac{-\psi(z)+\phi_p(z)}{U_T}\right) \text{ with}$$
$$qc = 1 - \frac{m_l^{3/2}}{m_l^{3/2}+m_h^{3/2}} \exp\left(-\zeta \frac{2m_l k_B T}{\hbar^2} z^2\right)$$
$$- \frac{m_h^{3/2}}{m_l^{3/2}+m_h^{3/2}} \exp\left(-\zeta \frac{2m_h k_B T}{\hbar^2} z^2\right), \quad (1)$$

where $n_{i,0}$ is the intrinsic density, qc the quantum correction factor, ψ the electrostatic potential and ϕ_p the quasi Fermi potential. The fitted light and heavy effective masses are $m_l = 0.235 m_0$ and $m_h = 0.255 m_0$. Using the function ζ, the IMLDA model can be matched to the reference data and the matching criterion is again the inversion charge density. In order to retain the computation time efficiency and the algorithm of the classical model for determination of the charge carrier density, ζ depends only on the distance from the interface, the temperature and the effective doping ($N_{eff} = |N_A - N_D|$):

$$\zeta(z, N_{eff}, T) = \frac{(z/z_n)^8 \cdot \zeta'(N_{eff}, T)}{(z/z_n)^3 + (z/z_n)^2 + (z/z_n) + 1}, \quad (2)$$

where $z_n = 1.5$ nm is a normalization constant. ζ' is a fitting function. The ansatz (2) separates the distance dependence in ζ from the temperature and doping dependencies, which are considered by ζ'. The problem now is to find an approximating function for the dependence on the temperature and doping of the function ζ'. The determination of ζ' consists of two steps. Firstly, discrete values to be matched by the function ζ' are evaluated by minimizing the deviations of the inversion density of the IMLDA model from the reference data for each temperature and doping. Finally, the computed set of discrete values for the function ζ' must be approximated by an analytic function of temperature and doping. For this purpose, the following functions are used

$$\zeta'(N_{eff}, T) = p_1 \left(\ln\left(\frac{\xi(N_{eff}) + 10^{17}/\text{cm}^3}{2 \cdot 10^{16}/\text{cm}^3}\right)\right)^{p_2} \cdot$$
$$\left(\frac{\xi(N_{eff}) - 7 \cdot 10^{17}/\text{cm}^3}{2 \cdot 10^{19}/\text{cm}^3} + 1\right)^{p_3} \cdot \left(\frac{T}{300\ \text{K}}\right)^{p_4} +$$
$$p_5 \cdot \ln^2\left(\frac{\xi(N_{eff})}{2.3 \cdot 10^{15}/\text{cm}^3}\right), \quad (3)$$

where $\xi(N_{eff})$ is given by

$$\xi(N_{eff}) = 5 \cdot 10^{16}/\text{cm}^3 \cdot F\left(\frac{N_{eff}}{5 \cdot 10^{16}/\text{cm}^3}\right) +$$
$$N_{eff} \cdot \left(F\left(\frac{N_{eff}}{5 \cdot 10^{18}/\text{cm}^3}\right) - F\left(\frac{N_{eff}}{5 \cdot 10^{16}/\text{cm}^3}\right)\right)$$
$$+ 5 \cdot 10^{18}/\text{cm}^3 \cdot \left(1 - F\left(\frac{N_{eff}}{5 \cdot 10^{18}/\text{cm}^3}\right)\right) \quad (4)$$
$$\text{with } F(x) = (1 + \exp(20 \cdot (x-1)))^{-1}. \quad (5)$$

Here p_1, p_2, p_3, p_4 and p_5 are the function parameters, which are shown in table 1.

Table 1: Determined parameters for equation (3)

p_1	p_2	p_3	p_4	p_5
0.4	0.482	2.353	2.887	0.0038

Note that in contrast to other simplified local models [3], [4], the IMLDA model developed here does not depend on the solution variables – electrostatic potential and quasi Fermi potential, whereby the convergence characteristics and computation time efficiency of the classical model without quantum corrections are maintained.

3 MOBILITY MODEL

The carrier mobility is approximated as proposed in [6] using a Matthiesen-like expression as follows:

$$\frac{1}{\mu} = \frac{1}{\mu_{\text{bulk}}} + \frac{1}{\mu_{\text{ac}}} + \frac{1}{\mu_{\text{sr}}}, \quad (6)$$

where μ_{bulk} is the bulk mobility, μ_{ac} the component due to surface acoustic phonons, and μ_{sr} the mobility limited by surface roughness scattering. In this work, the bulk mobility is described by the Klaasen model [13].

The second term in (6) due to surface acoustic phonons is modeled similarly to Ref. [6], [8]

$$\mu_{\text{ac}} = \frac{B}{E_\perp} + \frac{C \cdot C_{\text{mod}}(N_{eff})}{E_\perp^{1/3}} \cdot \left(\frac{300}{T}\right)^\kappa \quad (7)$$
$$\text{with } C_{\text{mod}}(N_{eff}) = \frac{a_1}{a_2 + a_3 \cdot \frac{N_{eff}^3}{N_{eff}^3 + N_1^3}}$$

The mobility limited by surface roughness scattering is given by

$$\mu_{\text{sr}} = \frac{\delta_{\text{mod}}(N_{eff})}{E_\perp^\gamma} \text{ with } \delta_{\text{mod}}(N_{eff}) = a_4 + \frac{a_5 \cdot N_{eff}^2}{N_{eff}^2 + N_2^2} \quad (8)$$

For the validation of the new model, mobility data from literature [14] as well as mobility data extracted from C(V) and I(V) measurements was used. The latter data was extracted for temperatures ranging from 273 K to 423 K and high channel doping using the method reported in [15]. In Figure 1 the extracted effective mobilities are compared with the mobility data of [14], showing good agreement in the corresponding ranges of electric field and temperature. The parameters of the new mobility model which were determined by matching these experimental data are given in table 2.

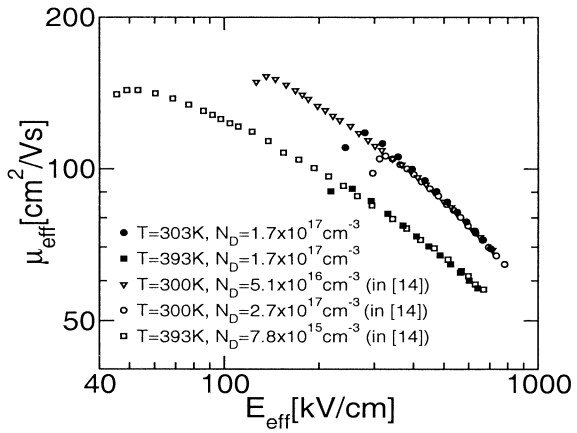

Figure 1: Comparison of the extracted effective hole mobility data to the data of Takagi [14] at different temperatures and channel dopings

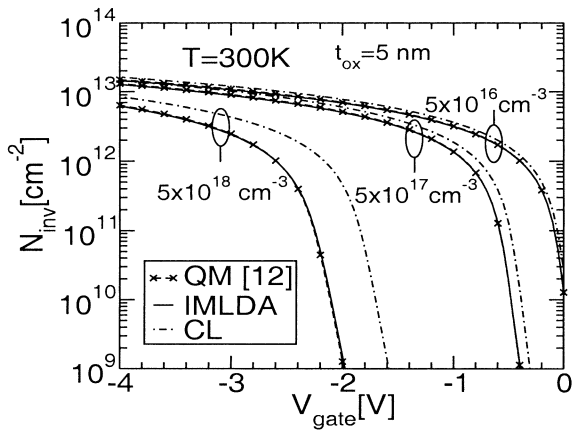

Figure 2: Inversion layer density N_{inv} for three doping concentrations at room temperature as a function of the gate voltage V_g for zero back bias V_b

Table 2: Parameters of the mobility model

B	$1.093 \cdot 10^7$	cm/s
C	$6.261 \cdot 10^3$	$\mathrm{cm}^{5/3}/\mathrm{V}^{2/3}\mathrm{s}$
κ	$9.933 \cdot 10^{-1}$	
γ	2.226	
N_1	$2.9 \cdot 10^{17}$	cm^{-3}
N_2	$2.8 \cdot 10^{17}$	cm^{-3}
$a1$	1.823	
$a2$	1.181	
$a3$	$3.1 \cdot 10^{-1}$	
$a4$	$3.944 \cdot 10^{15}$	V/s
$a5$	$3.454 \cdot 10^{15}$	V/s

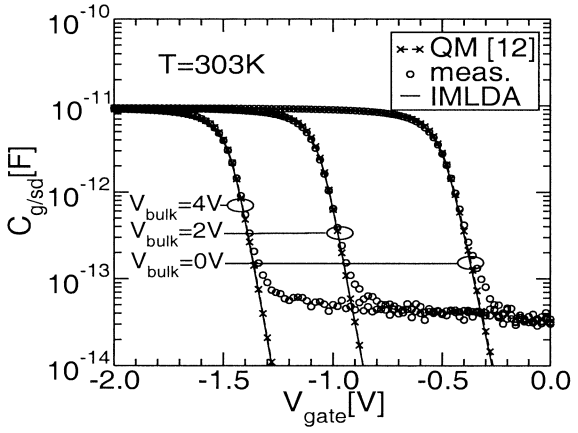

Figure 3: Gate-to-source/drain capacitance of a large gate area pMOSFET for a temperature of $303K$

4 RESULTS

Figure 2 illustrates the inversion charge density N_{inv} as a function of the gate voltage for three different homogeneous dopings. A very good agreement is found between the IMLDA and the quantum mechanical reference model (QM) [12], while, as expected, the classical model (CL) yields increasingly wrong results with higher channel dopings. Not only a threshold shift is found, but also a reduction of the capacitance.

Figure 3 shows the simulated and measured gate-to-source-drain capacitance at 303 K for a $50\mu\mathrm{m} \times 50\mu\mathrm{m}$-pMOSFET. The channel doping of the transistor is inhomogeneous and has a value of $1.7 \cdot 10^{17}/\mathrm{cm}^3$ at the $\mathrm{Si/SiO_2}$-interface. The oxide thickness is 7.5 nm and the gate material consists of highly doped p^+-poly silicon. The capacitances extracted from the IMLDA and the quantum mechanical model agree very well with the experimental results above the threshold voltage. The deviation between measurement and simulation in the subthreshold voltage results from the one dimensional approximation, which neglects the overlapping gate-to-source-drain capacitance.

In Figure 4 mobility modeling results are shown for different temperatures and different channel dopings. The new mobility model in conjunction with the IMLDA model reproduces the experimental results.

Figure 5 shows the input characteristics of the above described pMOSFET for three different bulk voltages. The simulations reproduce the measured drain current very well.

5 CONCLUSIONS

We have presented the first consistent and accurate combination of a quantum correction model for hole inversion layers and a hole channel mobility model, which is compatible to the quantum corrected spatial hole and field distributions in the channel. These models show excellent agreement with experimental data for a wide range of temperatures and

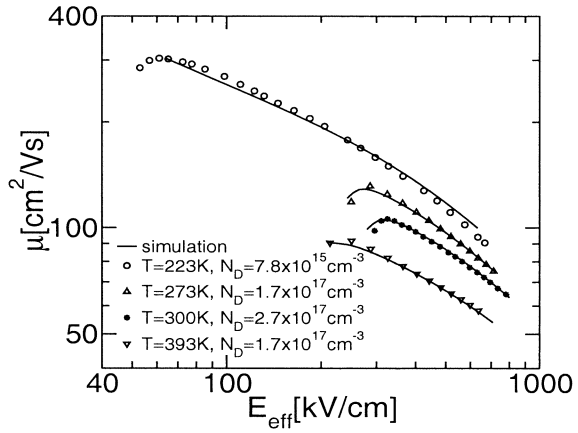

Figure 4: Effective inversion layer mobility μ_{eff} versus effective field E_{eff} simulated and measured

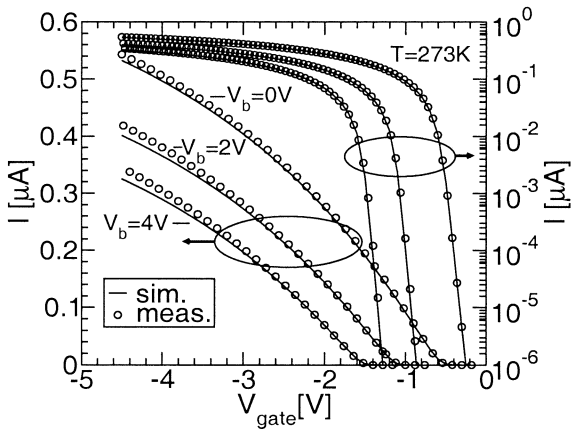

Figure 5: Drain current I_d versus gate voltage V_g for the 50μm-pMOSFET

channel doping concentrations. They are well suited for software implementation in existing TCAD device simulators.

6 ACKNOWLEDGMENTS

We'd like to thank the DFG for financial support under contract number ME 1590/1-3.

REFERENCES

[1] S. A. Hareland, S. Jallepalli, G. Chindalore, W. K. Shi, A. F. Tasch, and C. M. Maziar, "A simple model for quantum mechanical effects in hole inversion layer in silicon PMOS devices," *IEEE Trans. Electron Devices*, vol. 44, no. 8, pp. 1172–1173, 1997.

[2] C. S. Rafferty, B. Biegel, Z. Yu, M. C. Ancona, J. Bude, and R. W. Dutton, "Multi-dimensional quantum effect simulation using a density-gradient model and script-level programming techniques," in *Proc. SISPAD*, pp. 137–140, 1998.

[3] M. Ieong, R. Logan, and J. Slinkman, "Efficient quantum correction model for multi-dimensional CMOS simulations," in *Proc. SISPAD*, (Leuven (Belgium)), pp. 129–132, 1998.

[4] T. Usuki, T. Tanaka, S. Ohkubo, Y. Momiyama, T. Futatsugi, and T. Sugii, "Compact and accurate quantum correction for MOS device simulator," *IEDM Tech. Dig.*, pp. 531–534, 1999.

[5] C. Jungemann, C. D. Nguyen, B. Neinhüs, S. Decker, and B. Meinerzhagen, "Improved modified local density approximation for modeling of size quantization in NMOSFETs," in *MSM'2001*, (USA), pp. 458–461, 2001.

[6] M. N. Darwish, J. L. Lentz, M. R. Pinto, P. M. Zeitzoff, T. J. Krutsick, and H. H. Vuong, "An improved electron and hole mobility model for general purpose device simulation," *IEEE Trans. Electron Devices*, vol. 44, no. 9, pp. 1529–1538, 1997.

[7] S. Reggiani, M. Valdinoci, L. Colalongo, and G. Baccarani, "A unified analytical model for bulk and surface mobility in Si n- and p-channel MOSFET's," in *Proc. ESSDERC*, (Leuven (Belgium)), pp. 240–243, 1999.

[8] B. Neinhüs, C. D. Nguyen, C. Jungemann, and B. Meinerzhagen, "A CPU efficient electron mobility model for MOSFET simulation with quantum corrected charge densities," in *Proc. ESSDERC*, pp. 332–335, 2000.

[9] T. Ando, A. B. Fowler, and F. Stern, "Electronic properties of two-dimensional systems," *Rev. Mod. Phys.*, vol. 54, pp. 437–672, 1982.

[10] F. Stern, "Self-consistent results for n-type Si inversion layers," *Phys. Rev. B*, vol. 5, pp. 4891–4899, 1972.

[11] C. Jungemann, A. Emunds, and W. L. Engl, "Simulation of linear and nonlinear electron transport in homogeneous silicon inversion layers," *Solid–State Electron.*, vol. 36, pp. 1529–1540, 1993.

[12] R. Oberhuber, G. Zandler, and P. Vogl, "Subband structure and mobility of two-dimensional holes in strained Si/SiGe MOSFETs," *Phys. Rev. B*, vol. 58, pp. 9941–9948, 1998.

[13] D. B. M. Klaassen, "A unified mobility model for device simulation -I. Model equations and concentration dependence," *Solid–State Electron.*, vol. 35, pp. 953–959, 1992.

[14] S. Takagi, A. Toriumi, M. Iwase, and H. Tango, "On the universality of inversion layer mobility in si MOSFET's: Part I–Effects of substrate impurity concentration," *IEEE Trans. Electron Devices*, vol. 41, pp. 2357–2362, 1994.

[15] C. Jungemann, B. Meinerzhagen, and M. Eller, "On the number of fast interface states of standard CMOS technologies," *IEEE Electron Device Lett.*, vol. 20, no. 6, pp. 283–285, 1999.